

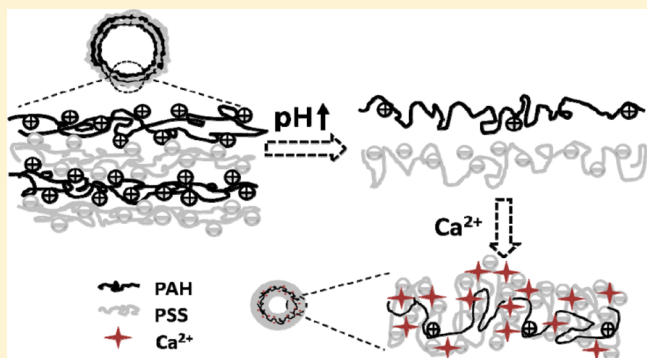
Phenomenon and Mechanism of Capsule Shrinking in Alkaline Solution Containing Calcium Ions

Shupeng She, Bowen Shan, Qinjin Li, Weijun Tong*, and Changyou Gao*

MOE Key Laboratory of Macromolecular Synthesis and Functionalization, Department of Polymer Science and Engineering, Zhejiang University, Hangzhou 310027, China

Supporting Information

ABSTRACT: Shrinking phenomenon of poly(allylamine hydrochloride) (PAH)/poly(styrene sulfonate, sodium salt) (PSS) multilayer microcapsules was observed when they were incubated in alkaline solutions containing Ca^{2+} . The shrinking was universal to those polyelectrolyte multilayer capsules regardless of the wall thickness and wall compositions suppose the conditions were proper. The shrinking extent increased along with the increase of solution pH and Ca^{2+} concentration, and reached to a maximum value of 70% (from 7.4 to 2.3 μm). The shrunk capsules with a hollow structure and thick wall could well maintain their spherical shape in a dry state. During the capsule shrinking partial loss of the polyelectrolytes especially PSS took place, and the loss amount increased along with the increase of solution pH although the alteration patterns were different at lower Ca^{2+} concentration. The complexation of PSS with Ca^{2+} , which is believed one of the major reasons governing the capsule shrinking, was demonstrated by X-ray photoelectron spectroscopy and turbidity experiment. The mechanism is proposed, which relies on the synergistic effects of deprotonation of PAH and screening of PSS by Ca^{2+} leading to the thermodynamically favored-capsule shrinking.



INTRODUCTION

The multilayer microcapsules fabricated via the layer-by-layer (LbL) assembly technique^{1–4} have shown various applications such as drug delivery carriers, biosensors, and reactors.^{5–9} The most overwhelming advantage of the multilayer microcapsules lies in the smart multiresponsiveness under environmental stimuli, emanating from many options of assembly driving forces,^{10–13} building blocks,^{3,14} and tunable mechanical properties.^{13,15} The stimuli-responsive properties have contributed much to the loading and controlled release of diverse substances, such as low-molecule-weight drugs,¹⁶ proteins,¹⁷ DNAs,¹⁸ and so forth in recent years.

Basically, the stimuli include salts,^{19–21} pH,^{22–24} light,^{25–27} temperature,^{16,20,28–31} magnetism,³² redox,^{33,34} and some special biomolecules^{35,36} leading to capsule disintegration, swelling, shrinking, and permeability alteration. The swelling and shrinking of the multilayer capsules is helpful to understand the basic physicochemical properties of the multilayer films because the hollow capsules possess free-standing structures and inner hollow space for rearrangement in three dimensions, which cannot be achieved by the flat counterparts adsorbed on a substrate. Furthermore, the shrinkage of capsules can be used to encapsulate various substances, which are released again in a controlled manner upon capsule swelling. Therefore, the swelling and shrinking behaviors of the microcapsules are of both fundamental and technical significance.

The capsule swelling and shrinking have been triggered by diverse stimuli. For instance, the PAH/PSS capsules templated on melamine formaldehyde (MF) particles or red blood cells shrunk to some extent upon annealing at 70 °C for 2 h.³¹ The PAH/PSS capsules could severely shrink to less than $\frac{1}{3}$ after annealed at 120 °C for 20 min,³⁰ and less shrunk to $\frac{4}{5}$ after incubated in a solution containing HCO_3^- or CO_3^{2-} for a couple of minutes.²¹ The PAH/PSS capsules also can be induced strong swelling after the interaction with some cationic surfactants (such as dodecyltrimethylammonium bromide and cetyltrimethylammonium bromide) but shrinking with benzalkonium chloride (BAC) as the cationic surfactant.³⁷ Redox-sensitive microcapsules based on hydrophobic force show reversible responsive swelling upon oxidation and shrinking after reduction.³⁴ Swelling and shrinking of poly(diallyldimethylammonium chloride) (PDADMAC)/PSS capsules in response to change in temperature and ionic strength were first observed by Gao et al.²⁰ and in the following more systematical studies it has been demonstrated that this behavior is determined by the outmost layer.^{28,29} Salt-induced reversible swelling–shrinking transition of PDADMAC/PSS capsules above their glass transition temperature was also observed.³⁸ Furthermore, a micromechanical theory was developed to

Received: August 9, 2012

Revised: October 25, 2012

Published: October 25, 2012

describe the experiments³⁸ as well as the pH-dependent swelling of PAH/poly(methacrylic acid) (PMA) microcapsules.³⁹

The PAH/PSS capsule is most widely investigated in the family of the polyelectrolyte capsules. They become swelling and then disintegrated in concentrated NaOH solution suggesting the instability of the PAH/PSS capsules at high pH.⁴⁰ Contrast to this result, in the presence of Ca²⁺ dramatic shrinkage of the PAH/PSS capsules in the alkaline solution is observed in this study. The synergistic effects of high pH and Ca²⁺ ions on the extents of capsule shrinkage are systematically and quantitatively studied. This capsule shrinking triggered by high pH and divalent ions is also observed for other polyelectrolyte capsules constructed from different building blocks. Finally, the mechanism is discussed and proposed.

■ EXPERIMENTAL SECTION

Materials. Poly(styrene sulfonate, sodium salt) (PSS, $M_w \sim 70$ kDa), poly(allylamine hydrochloride) (PAH, $M_w \sim 56$ kDa), poly(diallyldimethylammonium chloride) (PDADMAC, $M_w 200\text{--}350$ kDa), dextran sulfate (DS, $M_w \sim 100$ kDa), polyethyleneimine (PEI, $M_w \sim 750$ kDa), fluorescein and fluorescein isothiocyanate (FITC) were obtained from Sigma-Aldrich. Manganese sulfate ($MnSO_4$) was obtained from Shanghai Meixing Chemical Factory Co., Ltd. Ammonium hydrogen carbonate (NH_4HCO_3) and disodium ethylenediaminetetraacetate dihydrate (EDTA) were purchased from Guangdong Guanghua Chemical Factory Co., Ltd. Calcium chloride, sodium hydroxide, glutaraldehyde (GA), and barium chloride were purchased from Sinopharm Chemical Reagent Co., Ltd. All chemicals were used as received. The water used in all experiments was prepared in a Millipore Milli-Q Reference purification system. Spherical MnCO₃ microparticles were synthesized by mixing MnSO₄ and NH₄HCO₃ solutions according to reference.⁴¹

Microcapsule Preparation. Sequential adsorption of polyelectrolytes (2 mg·mL⁻¹) onto the MnCO₃ microparticles (~3% w/w in suspension) was conducted in 0.5 M NaCl solution for 10 min, followed by 3 washes in 0.5 M NaCl solution. The excess polyelectrolytes were removed by centrifugation at 1000 rpm for 1 min. After assembly of desired number of polyelectrolyte layers, the coated particles were incubated in 0.2 M EDTA solution (pH 7.0, adjusted by NaOH solution) for 30 min under shaking. The resultant capsules were washed with fresh EDTA solution thrice and finally washed thrice with water. FITC-labeled PAH or PEI (for the labeling protocol, ref 42) was used to build up the corresponding microcapsules for the visualization via confocal laser scanning microscopy (CLSM). The (PDADMAC/PSS)_{4.5} capsules were templated on CaCO₃ microparticles and were observed by adding little amount of fluorescein.

Cross-Linking of PAH/PSS Capsules. The PAH/PSS multilayer capsules were cross-linked by GA according to our previous report.⁴³ Briefly, the MnCO₃ microparticles coated with PAH/PSS multilayers were incubated in 2% GA solution at room temperature for 2 h, and then the particles were washed by water 3 times and the MnCO₃ templates were removed via the process mentioned above.

Preparation of Different Alkaline Solutions Containing Ca²⁺. Saturated Ca(OH)₂ solution was prepared and then diluted by water (5, 15, 20, 30, and 50 times) resulting in solutions with varied pH values and Ca²⁺ concentrations. For the solutions diluted by the same ratios, the Ca²⁺ concen-

trations were adjusted to 1, 5, 10, 50, and 100 mM by adding a small amount of CaCl₂ solution and their pH values were adjusted to same. All of the Ca(OH)₂ solutions were freshly prepared before use.

Shrinkage of Microcapsules. To investigate the factors affecting the shrinkage behavior of the (PAH/PSS)₅ microcapsules (7.4 ± 0.8 μm), 20 μL original microcapsule suspension (8.8×10^7 capsules/ml) was centrifuged at 4000 rpm for 3 min to discard the supernatant. Then 200 μL solution with fixed pH and Ca²⁺ concentration was added. After 5 min incubation under shaking, the capsules were centrifuged (4000 rpm, 3 min) to discard the supernatant and washed with water thrice for following characterizations. The shrinkage of the (PAH/DS)₅ and (PEI/PSS)₅ capsules in the alkaline solution (pH 11.2, Ca²⁺ 1 mM) were conducted in the same way. To test the effect of different divalent cations, 1.6 mM Ba(OH)₂ solution (pH 11.5) was used to treat the (PAH/PSS)₅ capsules too. The vessels containing the (PDADMAC/PSS)_{4.5} (PDADMAC as the outmost layer) capsules with and without 250 mM CaCl₂ were incubated in a water bath at 50 °C for 3 min, respectively.

Scanning Electron Microscopy (SEM). A drop of the capsules suspension was applied to a silicon wafer and dried in air overnight. After sputtered with gold, the sample was observed under HITACHI S-4800 instrument at an operation voltage of 3 keV.

Confocal Laser Scanning Microscopy (CLSM). A drop of the capsules suspension was applied to a cover slide and observed by Leica TCS SPS confocal scanning system equipped with a 100 \times oil immersion objective. To determine the capsule diameter, at least 200 capsules were analyzed by *Image J* software.

UV-vis Spectroscopy. Capsule suspension (100 μL , 1.6×10^8 capsules/ml) was centrifuged to discard the supernatant, and then 1 mL solution with desired pH and Ca²⁺ concentration was added. After 5 min incubation under shaking, the capsules were centrifuged (4000 rpm, 3 min) to collect the supernatant for UV-vis spectroscopy measurement (Shimadzu UV-vis 2550). The loss amount of PSS was obtained by referring to a calibration curve constructed at the corresponding pH. The total amount of PSS in 100 μL original microcapsules was quantified by dissolving all the capsules with NaOH (pH 12) and measured by UV-vis spectroscopy.

Transmission Electron Microscopy (TEM). The microcapsules typically shrunk to 2.3 ± 0.3 μm were washed with water thrice and then with graded ethanol/water solutions. The sample was embedded into epoxy resin and ultramicrotomed into thin sections, which were transferred onto a carbon film-coated copper grid and observed by a Philips Tecnal-10 TEM.

X-ray Photoelectron Spectroscopy (XPS). The calcium content in the microcapsules after shrinkage was detected by an Axis Ultra spectrometer (Kratos Analytical, U.K.) with a monochromated Al K α source at pass energies of 160 eV for survey spectra and 80 eV for core-level spectra.

■ RESULTS

It was disclosed that at room temperature the (PAH/PSS)₅ microcapsules swell and even disintegrate at higher pH (>11) due to the breakage of $-\text{NH}_3^+$ and $-\text{SO}_3^-$ ionic pairs and thereby the uncompensated repulsion force between PSS molecules.⁴⁰ In a similar alkaline solution, however, the (PAH/PSS)₅ microcapsules shrunk dramatically when the divalent Ca²⁺ cations were added (Figure 1). The shrinking extent

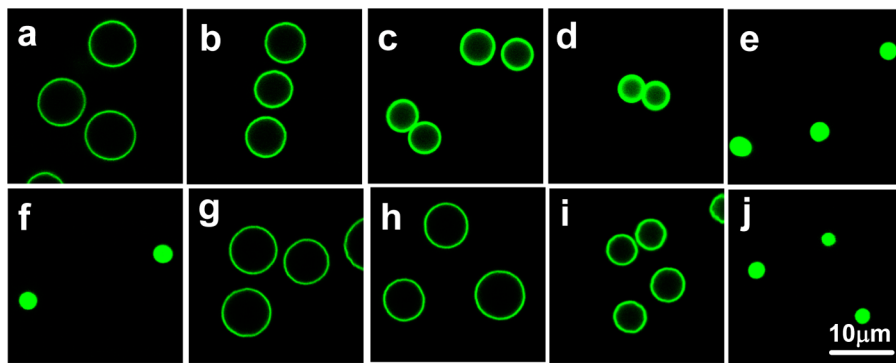


Figure 1. CLSM images of $(\text{PAH}/\text{PSS})_5$ capsules after incubation in alkaline solutions containing Ca^{2+} . In pH 11 solutions with the Ca^{2+} concentrations of (a) 0 mM, (b) 1 mM, (c) 5 mM, (d) 10 mM, (e) 50 mM, and (f) 100 mM, and in 10 mM Ca^{2+} solutions with the pH values of (g) 10.2, (h) 10.5, (i) 10.8, and (j) 11.4, respectively.

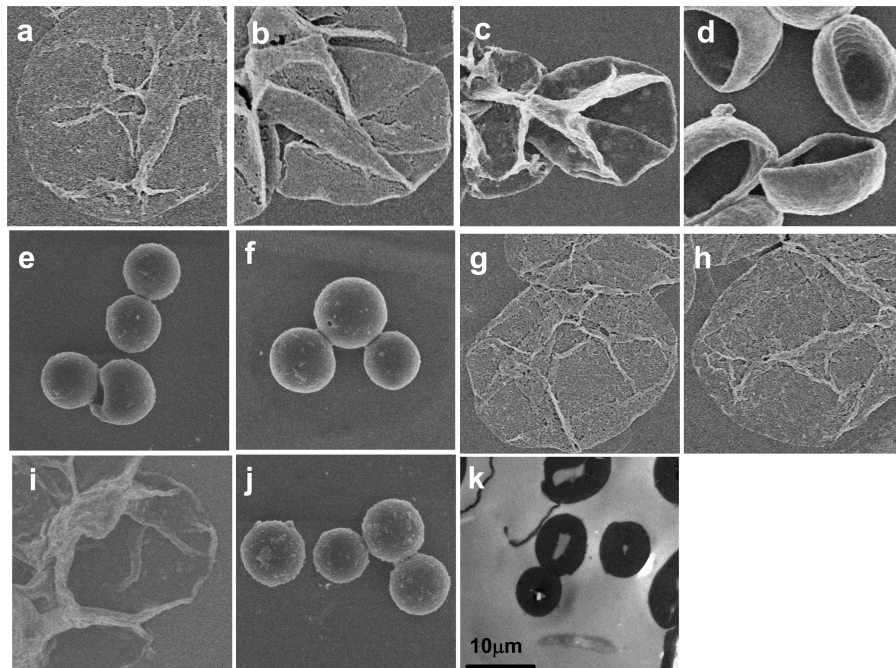


Figure 2. (a–j) SEM images of $(\text{PAH}/\text{PSS})_5$ capsules after incubation in alkaline solutions containing Ca^{2+} . In pH 11 solutions with the Ca^{2+} concentrations of (a) 0 mM, (b) 1 mM, (c) 5 mM, (d) 10 mM, (e) 50 mM, and (f) 100 mM, and in 10 mM Ca^{2+} solutions with the pH values of (g) 10.2, (h) 10.5, (i) 10.8, and (j) 11.4, respectively. (k) TEM image of an ultramicrotomed section of the sample shown in (f).

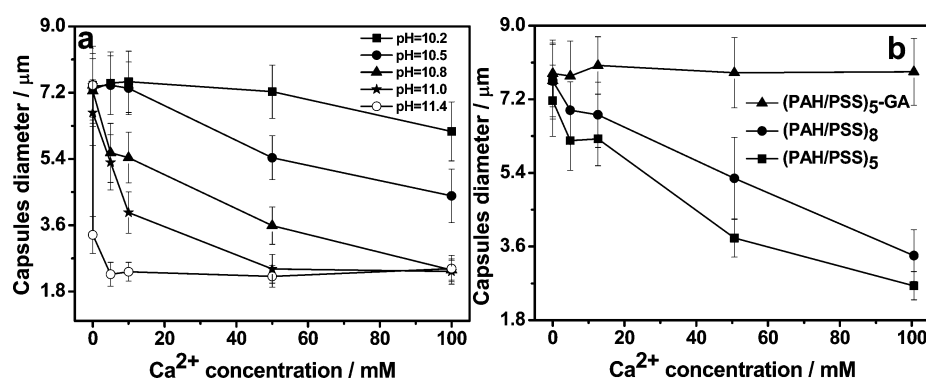


Figure 3. (a) Diameter of $(\text{PAH}/\text{PSS})_5$ capsules as a function of Ca^{2+} concentration at different pHs. (b) Diameter of different bilayer PAH/PSS capsules before and after GA cross-linking as a function of Ca^{2+} concentrations at pH 10.8. Data were obtained from CLSM images by averaging at least 200 capsules.

shows a positive correlation with the Ca^{2+} concentration and pH value. For example, at a fixed pH value of 11.0, the size of

the $(\text{PAH}/\text{PSS})_5$ capsules was gradually reduced from pristine $7.4 \pm 0.8 \mu\text{m}$ (part a of Figure 1) to $2.3 \pm 0.3 \mu\text{m}$ (part f of

Figure 1) when the Ca^{2+} concentration was increased from 0 to 100 mM. The largest shrinkage extent is near 70%. Moreover, at a fixed Ca^{2+} concentration of 10 mM the size of the capsules also gradually decreased to about $2.3 \pm 0.2 \mu\text{m}$ when the pH value was improved from 10.2 to 11.4 (parts g–j of Figure 1). The largest shrinkage extent is also about 70%. This value is significantly larger than that of the same capsules incubated in carbonate salts²¹ or annealed at high temperature (120 °C).³⁰ SEM observation found that the pristine capsules collapsed completely, forming the typical creases and folds (part a of Figure 2).² Along with the increase of Ca^{2+} concentration the creases and folds became higher on the capsules (parts b and c of Figure 2). A concave structure was formed in the dry state at 10 mM Ca^{2+} (part d of Figure 2) suggesting the thicker capsule walls.³⁴ The further shrunk capsules at Ca^{2+} concentrations of 50 and 100 mM maintained the spherical shape and smooth surface with a much smaller size (parts e and f of Figure 2). Nonetheless, small hollow cavity still existed inside the capsule (part k of Figure 2). At a fixed Ca^{2+} concentration, a similar alteration tendency of the capsule morphology and size was observed along with the increase of pH value (parts g–j of Figure 2).

Quantitative analysis confirms the above observation (Figure 3). Generally, the capsule size shows a decrease tendency along with the increase of Ca^{2+} concentration at each fixed pH value (part a of Figure 3). The reduction rate and final extent are positively dependent on the pH value. For example, at pH 10.2, the capsules can basically maintain their size even in 100 mM Ca^{2+} solution. By contrast, the capsule sharply shrunk to $2.3 \mu\text{m}$ at pH 11.4 even in a very low concentration of Ca^{2+} solution ($\leq 5 \text{ mM}$). The interplay between the Ca^{2+} concentration and pH value can well manipulate the capsule size between its pristine one ($7.4 \mu\text{m}$) and $2.3 \mu\text{m}$. Increase of the capsule wall thickness from 5 bilayers to 8 bilayers would not deter the capsule shrinking (part b of Figure 3), although the final shrinking extents were slightly reduced at each fixed Ca^{2+} concentration. Their size finally reached to $3.4 \pm 0.6 \mu\text{m}$, which is slightly larger than that ($2.6 \pm 0.3 \mu\text{m}$) of the 5 bilayer microcapsules treated at the same conditions. By contrast, the GA cross-linked (PAH/PSS)₅ microcapsules lost the ability of shrinking regardless of the Ca^{2+} concentration, which is consistent with the results observed previously.⁴³

The phenomenon of pH and Ca^{2+} triggered-capsule shrinking is not restricted to the PAH/PSS pairs but can also be applied to other capsules constructed from different polyelectrolytes pairs. For example, in a pH 11.2 solution containing 1 mM Ca^{2+} , the (PAH/DS)₅ and (PEI/PSS)₅ capsules shrunk from $7.1 \pm 0.6 \mu\text{m}$ (part a of Figure 4) and $7.0 \pm 0.6 \mu\text{m}$ (part b of Figure 4) to $2.9 \pm 0.3 \mu\text{m}$ (part d of Figure 4) and $3.2 \pm 0.5 \mu\text{m}$ (part e of Figure 4), respectively. Moreover, other divalent cations such as Ba^{2+} could similarly trigger the shrinking of (PAH/PSS)₅ capsules from $8.4 \pm 0.7 \mu\text{m}$ (part c of Figure 4) to $3.7 \pm 0.4 \mu\text{m}$ (part f of Figure 4) in a pH 11.5 solution containing 1.6 mM Ba^{2+} . Besides the polyanions shown here (PSS and DS containing $-\text{SO}_3^-$ or $-\text{SO}_4^-$), the microcapsules composed of PAH and PMA, which contains $-\text{COO}^-$ groups and has stronger complexation interactions with Ca^{2+} , also can shrink in the alkaline solution containing Ca^{2+} .⁴⁴ This result can further verify the universality of the process. However, the polyanions that form weaker or no complexes with Ca^{2+} are difficult to obtain. The fact⁴⁰ that the PAH/PSS capsules swell and disappear in the alkaline solution

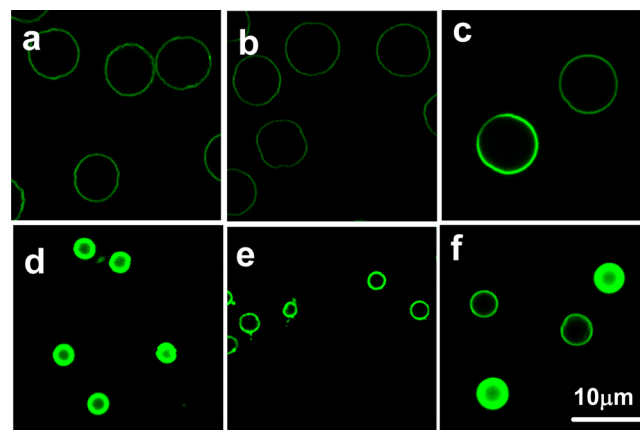


Figure 4. CLSM images show the shrinkage of different hollow polyelectrolyte multilayer capsules under different conditions. The (a,d) (PAH/DS)₅, (b,e) (PEI/PSS)₅, and (c,f) (PAH/PSS)₅ capsules before (a–c) and after incubated in solutions of (d,e) 1 mM Ca^{2+} , pH 11.2, and (f) 1.6 mM Ba^{2+} , pH 11.5, respectively.

without Ca^{2+} substantiates that the interaction between polyanions and Ca^{2+} is necessary for the shrinkage process.

The macroscopic swelling and shrinking of the microcapsules must rely on the rearrangement of the polyelectrolytes in the wall.²⁹ In this process partial loss of the polyelectrolytes may take place, and thereby was monitored by UV-vis spectroscopy. The validity of the method was testified first. The maximal released amount of PSS from the capsules was about 35% in the presence of excess Ca^{2+} . Taking the small amount of capsules and relatively large volume of bulk solution into account, the PSS concentration was as low as 0.05 mg/mL. In the presence of 100 mM CaCl_2 (the highest Ca^{2+} concentration used in our experiments), the solution is still quite clear without any turbidity. Then, the PSS absorbance in solution (0.05 mg/mL PSS containing 100 mM Ca^{2+}) at different pH (from neutral to as high as 11.5) was measured and compared with that of the solutions without Ca^{2+} . The absorbance almost kept constant with an error variance about 5%. Thus, it is reliable to use the UV-vis spectroscopy to quantify the PSS amount in the presence of Ca^{2+} .

The quantitative results of PSS mass loss were exhibited in part a of Figure 5. At all pH values, a significant amount of PSS (20–35%) was lost and kept unchanged when the Ca^{2+} concentration was higher than 10 mM, and a higher pH value resulted in a larger extent of PSS loss. The maximum loss amount of PSS is about 36% at pH 11.5. However, different patterns of PSS loss were observed when the pH value was lower or higher than 11.0. When the pH ≤ 11.0 the mass loss increased quickly until 10 mM Ca^{2+} and then leveled off. By contrast, at pH > 11.0 the mass loss was pretty high initially and then decreased slightly along with the increase of Ca^{2+} concentration. Accompanying with the PSS loss, some small amount of PAH was released too. For example, at pH 11.3 and 10 mM Ca^{2+} the loss mass of PAH (9.4%, from XPS) is only $1/3$ of that of the PSS (29.4%).

Because the experimental results demonstrate that the Ca^{2+} ions play a decisive role on the capsule shrinking, they must interact with the polyelectrolytes, here the most possible PSS molecules. According to the XPS results and the mass concentrations of N, S in PAH and PSS, the content of Ca element in the shrunk microcapsules was calculated (part b of Figure 5). At a fixed pH value, the amount of Ca^{2+} in the

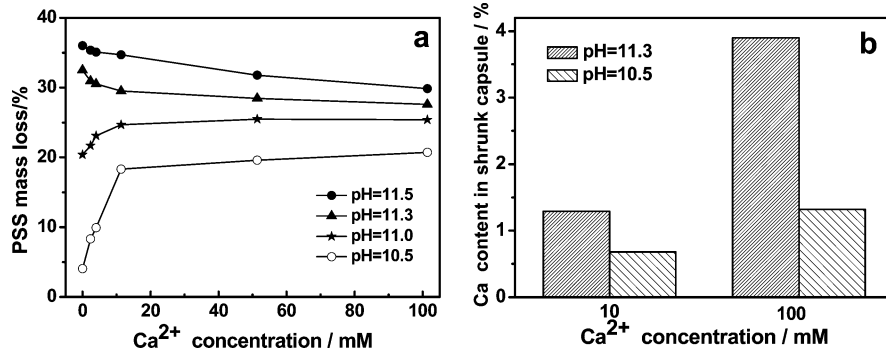


Figure 5. (a) Mass loss percentage of PSS from $(\text{PAH}/\text{PSS})_5$ capsules as a function of Ca^{2+} concentrations at different pHs. (b) Relative percentage of calcium element determined in the shrunk $(\text{PAH}/\text{PSS})_5$ microcapsules after treated at different Ca^{2+} concentration and pH value.

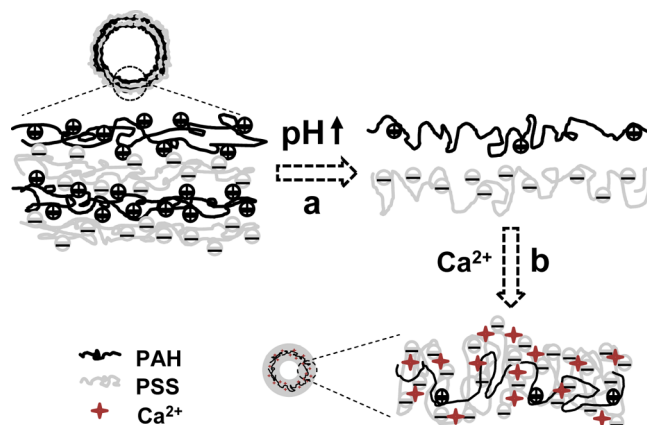
shrunk capsules increased along with the Ca^{2+} concentration. For example, at pH 11.3 the relative Ca^{2+} increased from 1.3% to 3.9% for the capsules treated with 10 mM and 100 mM Ca^{2+} solutions, respectively. Moreover, at a fixed Ca^{2+} concentration, a higher pH resulted in larger amount of Ca element in the capsules. It is worth mentioning that at 1 mM Ca^{2+} the relative amount of Ca element was too low to be detected by XPS. At neutral pH, no Ca^{2+} could be detected either on the capsules after incubation with even 100 mM CaCl_2 and 3 washes. Therefore, the high amount of Ca^{2+} combination cannot be contributed by the Ca^{2+} chelation as a result of EDTA adsorption in the capsule wall but by the large amount of free $-\text{SO}_3^-$ in the shell as a result of the higher pH value.

DISCUSSION

The polyelectrolyte multilayers are kinetically cross-linked and stabilized by the ionic bonds between a large numbers of oppositely charged groups in the polyelectrolytes. The multilayer capsules are generally stable at room temperature for a reasonable period of time. Annealing at higher temperature is a common method to improve the mobility of polymer chains allowing the rearrangement of the building blocks constituting the capsule wall.^{28–30} Moreover, the PAH/PSS capsules cannot survive in a solution with a pH value higher than 11 because of the deprotonation of $-\text{NH}_3^+$ groups and the electrostatic repulsion of the negatively charged $-\text{SO}_3^-$ groups.⁴⁰ In this case, both the PAH and PSS chains gain stronger enough mobility again. However, the current study found that on the contrary of swelling the $(\text{PAH}/\text{PSS})_5$ capsules shrink dramatically to 30% of their initial size after incubated in the alkaline solution containing Ca^{2+} . Therefore, the Ca^{2+} must come into play.

It is known that the $-\text{SO}_3^-$ group has a strong ability to complex with divalent cations such as Ca^{2+} used here, as revealed by the XPS characterization (part b of Figure 5). The ionic interaction is further intuitively demonstrated by the formation of opaque solution (part b of Figure S1 of the Supporting Information) upon both transparent solutions of CaCl_2 (part a of Figure S1 of the Supporting Information) and PSS were mixed. The ionic complexes could be destroyed by extraction of the Ca^{2+} ions via a stronger chelating agent, EDTA (part c of Figure S1 of the Supporting Information). The complexation of $-\text{SO}_3^-$ to Ca^{2+} causes at least the following two effects: (i) the charge repulsion between the $-\text{SO}_3^-$ groups in PSS chains is weakened and thereby the hydrophobicity of PSS chains is enhanced (Scheme 1), (ii) the PSS chains would adopt a more coiled conformation, which is known to induce

Scheme 1. Schematic Illustration to Show the Shrinkage Mechanism of Polyelectrolyte Microcapsule in an Alkaline Solution Containing Ca^{2+}



^a(a) Deprotonation of PAH in alkaline solution significantly reduces the number of ionic pairs between PAH and PSS, which in turn improves the mobility of the polyelectrolyte chains. (b) Complexation of Ca^{2+} and $-\text{SO}_3^-$ groups of PSS results in more coiled conformation and enhanced hydrophobicity of the capsule shell leading to the shrinkage and compaction of the capsule. These two processes should take place simultaneously in the system.

the shrinkage of capsules.⁴⁴ Meanwhile, the deprotonation of $-\text{NH}_3^+$ groups at high pH will make the PAH chains uncharged resulting in stronger hydrophobicity and more coiled conformation too (Scheme 1). As reported previously, shrinking or swelling of the capsules depends on the competition of surface tension as a result of an unfavorable polymer–solvent interaction and electrostatic repulsion as a result of the high excess charges in the capsule wall.^{28,29} In the alkaline solution containing divalent cations, the electrostatic repulsion is balanced, whereas the enhanced hydrophobicity and more coiled conformation of the polymer chains are beneficial to minimize the surface area, leading to the capsule shrinkage (Scheme 1). In summary, the alkaline solution deprotonates the PAH to some extent, and complexation of PSS with Ca^{2+} reduces the charge repulsion. The synergistic effects result in more coiled conformation of the polymer chains and improvement of the chain mobility leading to a more hydrophobic shell structure and thermodynamically favored-capsule shrinking. However, after the Ca^{2+} ions in the shrunk capsules were extracted by EDTA, the capsules still remained in the shrinking state (data not shown). This is

reasonable because the polyelectrolyte chains are in a frozen state and do not have enough mobility at room temperature and neutral pH, as also observed previously.⁴⁴

During the process of capsule shrinking, rearrangement of the polymer chains shall inevitably occur accompanying with the partial loss of the building blocks (part a of Figure 5). The uniform distribution of FITC-PAH in the final shrunk capsules (parts e, f, and j of Figure 1) verifies the chain rearrangement since the FITC-PAH layer was initially assembled on the last layer only. More solid proof is provided by the loss of shrinking ability of the cross-linked microcapsules (Figure 3), in which the PSS chains are entangled inside the network of the cross-linked PAH molecules. All of the results demonstrate that the chain rearrangement is indispensable for the capsule shrinking. This mechanism can easily explain the more severe capsule shrinking at higher pH values and Ca^{2+} concentrations because they are advantageous for either improving the deprotonation degree (for PAH) or screening the charge repulsion (for PSS), both resulting more coiled conformation of polymer chains.

The larger loss of PSS than that of PAH is attributed to its higher charge repulsion despite of partially screened by the calcium ions, and thereby easier dissolution into the alkaline solution, the reason for capsule disintegration in the absence of Ca^{2+} . At a fixed Ca^{2+} concentration, higher pH breaks more polyelectrolyte ionic pairs, leading to stronger chain mobility and thereby larger loss of PSS. The two different PSS loss patterns along with the increase of Ca^{2+} concentration (part a of Figure 5) can be explained as follows. At high pH values (pH 11.3 and 11.5) the PSS chains have stronger mobility and easily release from the capsule wall. The increase of Ca^{2+} concentration will form larger numbers of $-\text{SO}_3^-$ and Ca^{2+} complexes and enhance the hydrophobicity of the wall, reducing the PSS loss. At lower pH values (pH 11 and 10.5) the breakage of ionic pairs is not prominent. However, complexation of Ca^{2+} and $-\text{SO}_3^-$ would help to release the PSS chains^{45,46} leading to the increase of PSS loss along with the increase of Ca^{2+} concentration. But the total lost amount is apparently smaller than that at higher pH indicating that the mobility of the chains takes a more important role on the PSS loss.

According to the above discussion, the breakage of ionic bonds to generate the large enough number of free anionic sites for the divalent cation binding and the enhancement of the chain mobility in the multilayers are the prerequisites to induce the capsule shrinking. For this context, the generation of enough free anionic sites can be fulfilled by elevated temperature rather than the high pH for the PDADMAC/PSS capsules. The PDADMAC/PSS capsules with PDADMAC as the outmost layer swell significantly and even rupture after annealing.²⁹ As shown in Figure 6 compared to the pristine

(PDADMAC/PSS)₄PDADMAC ones (part a of Figure 6) the capsules expanded their size significantly after annealed at 50 °C for 3 min (part b of Figure 6). When 250 mM Ca^{2+} was added into the solution (part c of Figure 6) in contrast to the swelling the capsules shrunk from $8.5 \pm 0.9 \mu\text{m}$ to $4.4 \pm 0.6 \mu\text{m}$. Here, the elevated temperature takes the role like OH^- in the PAH/PSS system, decoupling some ionic bonds and leading to chain rearrangement,^{28,29} whereas the Ca^{2+} reduces the charge repulsion via complexation with PSS. Therefore, the proposed mechanism for the capsule shrinking can be further generalized and applied to other systems.

The shrinkage of capsules may be a useful way to tune the permeability of capsules⁴⁷ via the finely controlled shrinkage extent and thereby to encapsulate various functional substances.⁴⁸ However, the capsule permeability is not only dependent on the wall thickness but also the multilayer structures. The mass loss of both PSS and PAH during the shrinking process brings new component of Ca^{2+} and structure changes in the multilayers. Therefore, further experiments should be performed to clarify the permeability change and ability to encapsulate substances.

CONCLUSIONS

The shrinking phenomenon of polyelectrolyte multilayer microcapsules, typically represented by the pairs of (PAH/PSS)₅, in alkaline solution containing Ca^{2+} have been found and systematically studied. The synergistic effects of pH value and Ca^{2+} concentration determine the shrinkage extent of the capsules. The size of the capsules decreases gradually along with the increase of Ca^{2+} concentration at a given pH or the pH value at a given Ca^{2+} concentration. Unlike the fully collapsed morphology of the pristine ones, the highly shrunk capsules can well maintain their spherical shapes in a dry state. The capsule shrinking is a universal phenomenon regardless of the wall thickness and wall compositions suppose the conditions are proper. During the capsule shrinking process, partial loss of PSS takes place, whose amount is 3 times of that of PAH and increases along with the pH increase. On the basis of the experimental results, the mechanism is clarified. Briefly, the alkaline solution deprotonates the PAH to some extent, and complexation of PSS with Ca^{2+} reduces the charge repulsion. The synergistic effects result in more coiled conformation of the polymer chains and improvement of the chain mobility leading to a more hydrophobic shell structure and thermodynamically favored capsule shrinking. Using this mechanism, the (PDADMAC/PSS)₄PDADMAC capsules that originally show a swelling behavior at elevated temperature are shrunk in the presence of Ca^{2+} .

ASSOCIATED CONTENT

Supporting Information

Photos of solutions of CaCl_2 , CaCl_2/PSS , and $\text{CaCl}_2/\text{PSS}/\text{EDTA}$. This material is available free of charge via the Internet at <http://pubs.acs.org>.

AUTHOR INFORMATION

Corresponding Author

*E-mail: tongwj@zju.edu.cn (W.T.); cygao@mail.hz.zj.cn (C.G.), Tel/Fax: +86-571-87951108.

Notes

The authors declare no competing financial interest.

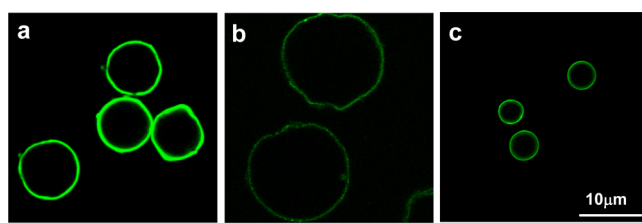


Figure 6. CLSM images of (PDADMAC/PSS)₄PDADMAC capsules before (a) and after treatments at 50 °C for 3 min without (b) and with 250 mM Ca^{2+} (c), respectively.

ACKNOWLEDGMENTS

This study is financially supported by the Natural Science Foundation of China (Nos. 21174130 and 51120135001), the Ministry of Science and Technology of China for the Indo-China Cooperation (2010DFA51510), Zhejiang Provincial Natural Science Foundation of China (Z4090177 and Y4110064), and Open Project of State Key Laboratory of Supramolecular Structure and Materials (sklssm201224).

REFERENCES

- (1) Peyratout, C. S.; Dähne, L. *Angew. Chem., Int. Ed.* **2004**, *43*, 3762–3783.
- (2) Donath, E.; Sukhorukov, G. B.; Caruso, F.; Davis, S. A.; Möhwald, H. *Angew. Chem., Int. Ed.* **1998**, *37*, 2202–2205.
- (3) Caruso, F.; Caruso, R. A.; Möhwald, H. *Science* **1998**, *282*, 1111–1114.
- (4) Sukhorukov, G. B.; Donath, E.; Lichtenfeld, H.; Knippe, E.; Knippe, M.; Budde, A.; Möhwald, H. *Colloids Surf, A* **1998**, *137*, 253–266.
- (5) McShane, M.; Ritter, D. *J. Mater. Chem.* **2010**, *20*, 8189–8193.
- (6) Sukhorukov, G. B.; Rogach, A. L.; Garstka, M.; Springer, S.; Parak, W. J.; Munoz-Javier, A.; Kreft, O.; Skirtach, A. G.; Susha, A. S.; Ramaye, Y.; Palankar, R.; Winterhalter, M. *Small* **2007**, *3*, 944–955.
- (7) Sukhorukov, G. B.; Rogach, A. L.; Zebl, B.; Liedl, T.; Skirtach, A. G.; Köhler, K.; Antipov, A. A.; Gaponik, N.; Susha, A. S.; Winterhalter, M.; Parak, W. J. *Small* **2005**, *1*, 194–200.
- (8) Tong, W. J.; Gao, C. Y. *J. Mater. Chem.* **2008**, *18*, 3799–3812.
- (9) Tong, W. J.; Song, X. X.; Gao, C. Y. *Chem. Soc. Rev.* **2012**, *41*, 6103–6124.
- (10) Such, G. K.; Quinn, J. F.; Quinn, A.; Tjipto, E.; Caruso, F. *J. Am. Chem. Soc.* **2006**, *128*, 9318–9319.
- (11) Such, G. K.; Johnston, A. P. R.; Caruso, F. *Chem. Soc. Rev.* **2011**, *40*, 19–29.
- (12) Wang, Z. P.; Feng, Z. Q.; Gao, C. Y. *Chem. Mater.* **2008**, *20*, 4194–4199.
- (13) Feng, Z. Q.; Wang, Z. P.; Gao, C. Y.; Shen, J. C. *Adv. Mater.* **2007**, *19*, 3687–3691.
- (14) Itoh, Y.; Matsusaki, M.; Kida, T.; Akashi, M. *Biomacromolecules* **2006**, *7*, 2715–2718.
- (15) She, S. P.; Xu, C. X.; Yin, X. F.; Tong, W. J.; Gao, C. Y. *Langmuir* **2012**, *28*, 5010–5016.
- (16) Tong, W. J.; She, S. P.; Xie, L. L.; Gao, C. Y. *Soft Matter* **2011**, *7*, 8258–8265.
- (17) De Temmerman, M. L.; Demeester, J.; De Vos, F.; De Smedt, S. *C. Biomacromolecules* **2011**, *12*, 1283–1289.
- (18) Borodina, T.; Markvicheva, E.; Kunizhev, S.; Moehwald, H.; Sukhorukov, G. B.; Kreft, O. *Macromol. Rapid Commun.* **2007**, *28*, 1894–1899.
- (19) Ibarz, G.; Dahne, L.; Donath, E.; Möhwald, H. *Adv. Mater.* **2001**, *13*, 1324–1327.
- (20) Gao, C. Y.; Leporatti, S.; Moya, S.; Donath, E.; Möhwald, H. *Chem.—Eur. J.* **2003**, *9*, 915–920.
- (21) Georgieva, R.; Dimova, R.; Sukhorukov, G.; Ibarz, G.; Möhwald, H. *J. Mater. Chem.* **2005**, *15*, 4301–4310.
- (22) Mauser, T.; Dejugnat, C.; Sukhorukov, G. B. *Macromol. Rapid Commun.* **2004**, *25*, 1781–1785.
- (23) Sukhorukov, G. B.; Antipov, A. A.; Voigt, A.; Donath, E.; Möhwald, H. *Macromol. Rapid Commun.* **2001**, *22*, 44–46.
- (24) Gao, C. Y.; Möhwald, H.; Shen, J. C. *Adv. Mater.* **2003**, *15*, 930–933.
- (25) Skirtach, A. G.; Javier, A. M.; Kreft, O.; Köhler, K.; Alberola, A. P.; Möhwald, H.; Parak, W. J.; Sukhorukov, G. B. *Angew. Chem., Int. Ed.* **2006**, *45*, 4612–4617.
- (26) Radt, B.; Smith, T. A.; Caruso, F. *Adv. Mater.* **2004**, *16*, 2184–2189.
- (27) Skirtach, A. G.; Antipov, A. A.; Shchukin, D. G.; Sukhorukov, G. B. *Langmuir* **2004**, *20*, 6988–6992.
- (28) Köhler, K.; Möhwald, H.; Sukhorukov, G. B. *J. Phys. Chem. B* **2006**, *110*, 24002–24010.
- (29) Köhler, K.; Shchukin, D. G.; Möhwald, H.; Sukhorukov, G. B. *J. Phys. Chem. B* **2005**, *109*, 18250–18259.
- (30) Köhler, K.; Shchukin, D. G.; Sukhorukov, G. B.; Möhwald, H. *Macromolecules* **2004**, *37*, 9546–9550.
- (31) Leporatti, S.; Gao, C.; Viogt, A.; Donath, E.; Möhwald, H. *Eur. Phys. J. E* **2001**, *5*, 13–20.
- (32) Lu, Z. H.; Prouty, M. D.; Guo, Z. H.; Golub, V. O.; Kumar, C. S. S. R.; Lvov, Y. M. *Langmuir* **2005**, *21*, 2042–2050.
- (33) Ma, Y. J.; Dong, W. F.; Hempenius, M. A.; Möhwald, H.; Vancso, G. J. *Nat. Mater.* **2006**, *5*, 724–729.
- (34) Wang, Z. P.; Möhwald, H.; Gao, C. Y. *Langmuir* **2011**, *27*, 1286–1291.
- (35) Zhu, Y.; Tong, W. J.; Gao, C. Y. *Soft Matter* **2011**, *7*, 5805–5815.
- (36) Ochs, C. J.; Such, G. K.; Yan, Y.; van Koeverden, M. P.; Caruso, F. *ACS Nano* **2010**, *4*, 1653–1663.
- (37) Kang, J.; Dähne, L. *Langmuir* **2011**, *27*, 4627–4634.
- (38) Köhler, K.; Biesheuvel, P. M.; Weinkamer, R.; Möhwald, H.; Sukhorukov, G. B. *Phys. Rev. Lett.* **2006**, *97*, 18830 1–4.
- (39) Biesheuvel, P. M.; Mauser, T.; Sukhorukov, G. B.; Möhwald, H. *Macromolecules* **2006**, *39*, 8480–8486.
- (40) Dejugnat, C.; Sukhorukov, G. B. *Langmuir* **2004**, *20*, 7265–7269.
- (41) Tong, W. J.; Gao, C. Y. *Colloids Surf, A* **2007**, *295*, 233–238.
- (42) Tong, W. J.; Gao, C. Y.; Möhwald, H. *Macromol. Rapid Commun.* **2006**, *27*, 2078–2083.
- (43) Tong, W. J.; Gao, C. Y.; Möhwald, H. *Chem. Mater.* **2005**, *17*, 4610–4616.
- (44) Mauser, T.; Dejugnat, C.; Möhwald, H.; Sukhorukov, G. B. *Langmuir* **2006**, *22*, 5888–5893.
- (45) Wang, T. X.; Colfen, H.; Antonietti, M. *J. Am. Chem. Soc.* **2005**, *127*, 3246–3247.
- (46) Sinn, C. G.; Dimova, R.; Antonietti, M. *Macromolecules* **2004**, *37*, 3444–3450.
- (47) Ibarz, G.; Dahne, L.; Donath, E.; Möhwald, H. *Chem. Mater.* **2002**, *14*, 4059–4062.
- (48) Köhler, K.; Sukhorukov, G. B. *Adv. Funct. Mater.* **2007**, *17*, 2053–2061.